Journal of Colloid and Interface Science 504 (2017) 305–314

Contents lists available at ScienceDirect

Journal of Colloid and Interface Science

journal homepage: www.elsevier.com/locate/jcis

Regular Article

Tailoring the multi-functionalities of one-dimensional ceria nanostructures via oxygen vacancy modulation

Haiwei Du [a], Tao Wan [a], Bo Qu [a], Jason Scott [b], Xi Lin [a], Adnan Younis [a], Dewei Chu [a,*]

[a] School of Materials Science and Engineering, University of New South Wales, Sydney, NSW 2052, Australia
[b] Particles and Catalysis Research Group, School of Chemical Engineering, University of New South Wales, Sydney, NSW 2052, Australia

GRAPHICAL ABSTRACT

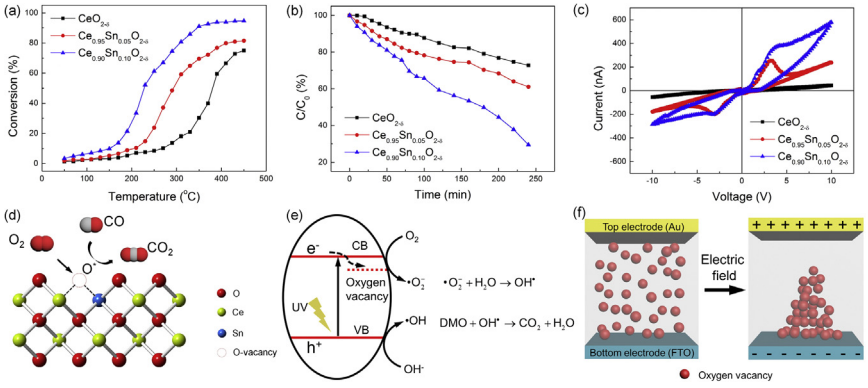

ARTICLE INFO

Article history:
Received 6 April 2017
Revised 16 May 2017
Accepted 17 May 2017
Available online 21 May 2017

Keywords:
CeO_2 nanostructure
Oxygen vacancy
Catalytic properties
Resistance switching

ABSTRACT

Lattice defects, for example oxygen vacancies in cerium oxide (CeO_2), usually play a vital role in determining physical and chemical properties, including catalytic performance and resistance switching behaviour. Here, tin (Sn) was introduced as a dopant in one dimensional CeO_2 nanostructures to investigate oxygen vacancy modulation and achieve improved catalytic properties and a tunable electrical performance. Our findings revealed that the Sn-doped CeO_2 nanorods maintained their morphology while the aspect ratio decreased gradually with increasing Sn content. The variation in oxygen vacancy concentration with Sn doping was confirmed by Raman and X-ray photoelectron spectroscopies and enhanced thermal catalytic and photo-catalytic performances were attained for the Sn-doped CeO_2 nanorods. The variation in oxygen vacancy concentration with Sn doping was also found to influence its electrical properties. Hysteresis loops expressing resistance switching behaviour were observed in Sn-doped $CeO_{2-\delta}$ nanorods. The results detailed in this study can help to rationally design nanostructures with the potential to provide desirable multi-functionalities.

1. Introduction

With the significant progress of nanotechnology, the past decades have witnessed the great potential of metal oxide semiconductor nanomaterials for catalytic applications. Generally, the unique characteristics of nanocrystals emerged from their size effect and morphology dependence. It is believed that, by reducing the size of nanocrystals, high surface to volume ratios can be achieved which are more effective for catalysis than their bulk counterparts. Additionally, the catalytic properties of nanocrystals also possess a strong shape/morphology-dependency [1,2]. The

* Corresponding author.
E-mail address: d.chu@unsw.edu.au (D. Chu).

http://dx.doi.org/10.1016/j.jcis.2017.05.057
0021-9797/

designed morphology can ensure a selective exposure of actively reactive facets with a specific surface atomic arrangement and coordination to generate more active sites [3]. Among various nanostructures, one-dimensional (1-D) nanocrystals usually exhibit superior performances for catalytic applications as they both share certain common characteristics (such as quantum size effect and large specific surface area) with 0-D nanoparticles and 2-D nanosheets and can achieve the 1-D carrier transport efficiently [4]. As a consequence of these advantages, many metal oxides with rod-like morphologies have shown outstanding and exceptional catalytic activities with greater stability [3].

Another superiority of metal oxide nanomaterials is their capacity for defect engineering [5], which is frequently applied to tailor and further modify their material properties. In particular, as a representative lattice defect in metal oxides, oxygen vacancies unquestionably play a critical role in modulating either thermocatalytic (e.g. carbon monoxide (CO) oxidation) [6] or photocatalytic activities [7]. They can act as active sites to promote CO oxidation by facilitating oxygen migration or provide enhanced photocatalytic efficiencies whereby the oxygen vacancies within the structure can serve as electron traps to inhibit electron-hole pair recombination [8].

Cerium oxide (CeO_2) nanocrystals have been widely studied as catalysts [9] or catalyst supports [10] (for example, metal particles) as they are recognized to possess extraordinary redox properties and a strong oxygen storage capacity (OSC) in nature. The intrinsic redox behaviour originates from the charge transfer between two oxidation states (Ce^{3+}/Ce^{4+}), consequently producing an oxygen-deficient form, $CeO_{2-\delta}$, which is rich in oxygen vacancies and can more easily chemisorb and activate molecular oxygen compared with the stoichiometric CeO_2 [11]. Generally, the concentration of oxygen vacancies in CeO_2 nanomaterials can be modulated by three approaches: morphology design, doping or thermal annealing in a reducing atmosphere. The former two approaches have gained more attention from the scientific community in the field of nanocrystals synthesis. Firstly, with a cubic fluorite structure, the morphology evolution of CeO_2 nanocrystals is usually associated with selectively exposed facets. As the formation energy of oxygen vacancies follows the sequence: (100) < (110) < (111) [12], structures with a {100}/{110}-dominated surface are catalytically more reactive for CO oxidation [13]. That is, nanorods preferentially exposing {100} and {110} facets with a higher OSC exhibit a better catalytic performance than nanocubes with only {100} facets or nano-octahedrons with only {111} facets, respectively [14]. Secondly, cation substitution with trivalent acceptor dopants possessing a similar ionic radius is often utilized to generate more oxygen vacancies in the lattice structure [15]. This strategy, based on forming oxygen vacancies induced by an extrinsic dopant, is designed to maintain charge neutrality. Additionally, doping is beneficial for band gap tuning, further facilitating photocatalytic efficiency. Among the many dopants, tin (Sn) has been shown to theoretically lower the formation energy of oxygen vacancies by electronic modification and structural distortion [16], and also experimentally to enhance the CO catalytic properties [17]. Despite the perceived benefits, and to the best of our knowledge, there currently are limited reports available on Sn-doped CeO_2 1-D nanostructures which examine their catalytic properties.

In this work, 1-D Sn-doped $CeO_{2-\delta}$ nanorods are synthesized by a hydrothermal method and the effects of Sn doping on morphology, crystal structure and especially the oxygen vacancy concentration are studied. As the amount of Sn increases, $Ce_{1-x}Sn_xO_{2-\delta}$ is found to maintain its rod-like morphology although the length to diameter (L/D) ratio decreases. Additionally, doping Sn into the ceria lattice enhanced the oxygen vacancy concentration, which was confirmed by Raman and XPS spectra. The Sn-doped $CeO_{2-\delta}$ nanorods exhibited better catalytic CO oxidation and photocatalytic performances as compared to neat ceria. Furthermore, as the resistance switching (RS) behaviour in metal oxides is typically accompanied by the migration of oxygen vacancies [18] the RS characteristics of the $Ce_{1-x}Sn_xO_{2-\delta}$ nanorods were investigated, to further reveal the role of oxygen vacancies on performance.

2. Experimental procedure

2.1. Materials

Cerium chloride heptahydrate ($CeCl_3{\cdot}7H_2O$, M_w: 372.58), tin(II) acetate ($SnC_4H_6O_4$, M_w: 236.80) 1,2-propanediol (ρ: 1.036 g/mL), acetic acid (CH_3COOH, M_w: 60.05) and ammonia hydroxide solution (ρ: 0.9 g/mL). All chemicals were purchased from Sigma-Aldrich and used without further purification.

2.2. Synthesis of $Ce_{1-x}Sn_xO_{2-\delta}$ nanorods (x = 0, 0.05 and 0.10)

To obtain $CeO_{2-\delta}$ nanorods, 0.3 M $CeCl_3{\cdot}7H_2O$ was dissolved in 5 mL deionized (DI) water after which 100 μL acetic acid and 15 mL 1,2-propanediol were added into the solution in that order. For the synthesis of $Ce_{1-x}Sn_xO_{2-\delta}$ nanorods, $CeCl_3{\cdot}7H_2O$ and $SnC_4H_6O_4$ were weighed stoichiometrically without using acetic acid. After stirring for 5 min, 10 mL of ammonia hydroxide solution was added dropwise to the mixed solution under magnetic stirring, whereby the colour of the solution turned to light orange. After stirring for 30 min, the solution was transferred into a Teflon flask which was sealed tightly in a stainless-steel autoclave. Hydrothermal treatment was conducted at 160 °C for 12 h. After cooling, the white precipitate was collected and washed with DI water and then centrifuged at 5000 rpm for 2 min for five cycles, and then dried in an oven at 70 °C for 24 h.

2.3. Fabrication of FTO/$Ce_{1-x}Sn_xO_{2-\delta}$/Au devices

The as-prepared $Ce_{1-x}Sn_xO_{2-\delta}$ nanorods were dispersed into 5 mL of ethanol with assistance of ultrasound for 5 min. Afterwards, the suspension was drop-coated (a drop of 10 μL) once onto FTO glass, which acted as the bottom electrode, to provide a self-assembled film. The film was dried in an oven at 75 °C for 2 min. Finally, a patterned Au electrode with a size of ~250 μm in diameter was sputtered through a shadow mask onto the film surface to act as the top electrode.

2.4. Materials characterization

Structural analysis of the as-synthesized $Ce_{1-x}Sn_xO_{2-\delta}$ nanorods was performed using an X-ray diffractometer with Cu Kα radiation (λ = 0.1541 nm). The microstructures were visually observed by transmission electron microscopy, TEM (FEI Tecnai G2 and Philips CM200). Raman spectra were collected on a Renishaw inVia Raman Microscope with a 514 nm laser. The band gap was calculated by measuring the absorption spectra using a PerkinElmer UV–Visible Spectrometer. The chemical bonding states were investigated by X-ray photoelectron spectroscopy, XPS (ESCALAB250Xi spectrometer). The specific surface area (SSA) was determined by the Bru nauer–Emmett–Teller (BET) method using a Micromeritics ASAP 2000 Gas Sorption Analyser. The current-voltage (*I-V*) characteristics of the FTO/$Ce_{1-x}Sn_xO_{2-\delta}$/Au devices were tested by a Keysight B2902A source-meter.

2.5. H_2-temperature-programmed reduction (H_2-TPR) measurements

the samples were analysed on a Micromeritics Autochem II. Approximately 100 mg of sample was added to a quartz U-cell